Molecular Therapy
Oncolytics
Original Article

Oncolytic adenovirus inhibits malignant ascites of advanced ovarian cancer by reprogramming the ascitic immune microenvironment

Gang Shi,[1] Pengyi Shi,[1] Yan Yu,[1] Jia Xu,[1] Jinhu Ma,[1] Yong Zhang,[1] Zhexu Dong,[1] Lanlin Shen,[1] Lei Dai,[1] Lin Cheng,[1] Ping Cheng,[1] and Hongxin Deng[1]

[1]State Key Laboratory of Biotherapy and Cancer Center, Collaborative Innovation Center of Biotherapy, West China Hospital, Sichuan University, Ke-yuan Road 4, No. 1, Gao-peng Street, Chengdu, Sichuan 610041, P.R. China

Malignant ascites frequently occur in patients with advanced ovarian cancer at initial diagnosis, and in almost all cases of relapse, they are closely related to poor prognosis, chemoresistance, and metastasis. To date, effective management strategies have been limited. In this study, we aimed to investigate the effects of oncolytic adenovirus (OV) on malignant ascites in a mouse model of advanced ovarian cancer. The results suggested that OV conferred an effective ability to reduce ascites development and prolong overall survival. Further analysis of the ascitic immune microenvironment revealed that OV treatment promoted T cell infiltration, activation, and differentiation into the effector phenotype; reprogrammed macrophages toward the M1-like phenotype; and increased the ratios of both $CD8^+$ T cells to $CD4^+$ T cells and M1 to M2 macrophages. However, immunosuppressive factors such as PD-1, LAG-3, and Tregs emerged after treatment. Combination therapy including OV, CSF-1R inhibitor PLX3397, and anti-PD-1 remarkably delayed the progression of ascites, and combination therapy induced a greater extent of T cell infiltration, proliferation, and activation. This study provides experimental and theoretical evidence for oncolytic virus-based treatment of malignant ascites, which may further contribute to advanced ovarian cancer therapy.

INTRODUCTION

Malignant ascites are present in more than one-third of ovarian cancer patients.[1,2] As a comorbidity, the emergence of malignant ascites can have a significant impact on a patient's quality of life, causing abdominal distension, pain, nausea, and impaired movement.[3] In addition, malignant ascites are closely associated with poor prognosis, relapse, drug resistance, and metastasis.[4–6] The larger volume of ascites accumulation was consistent with shorter progression-free survival (PFS) in a large study of 685 patients, in which patients with ascites volume >2 L demonstrated shorter PFS and overall survival (OS).[7] Ascites could be an independent prognostic indicator, considering that more than 90% of ovarian cancer patients with malignant ascites are diagnosed with stage III and IV cancer.[8,9] Immune cells and cytokines are important components of malignant ascites and are associated with disease progression.[6] Previous studies have shown that the immunoreactive phenotype is consistent with lower ascites volume.[10,11] Patients with a higher ratio of CD8/CD4 and effector T cells in ascites had longer PFS,[11,12] indicating that a strong immune response might be essential to overcome ovarian cancer-induced ascites. At present, no therapeutic strategy has been applied to standard practice to manage or prevent ascites secondary to ovarian cancer; paracentesis is generally used to attenuate ascites and their symptoms, and anti-angiogenic therapy via vascular endothelial growth factor (VEGF) inhibition is currently emerging as a potential approach. Nevertheless, the side effects are obvious, and new and effective strategies are required.

Oncolytic viruses have emerged as a promising approach in the field of cancer therapy, based on their extensive effects, including direct oncolysis, release of tumor-associated antigens (TAAs), and induction of immune cell infiltration.[13–15] Systemic antitumor effects could be achieved by local injection of oncolytic viruses, whereby TAAs released by local or intratumoral injection of oncolytic adenovirus (OV) could act as a vaccine *in situ* to activate the immune system and recruit immune cells into the tumor microenvironment,[16,17] thus shifting "cold" tumors to "hot" tumors and being key to successful immunotherapy in tumors with low immune scores.[18] These advantages resulted in the approval of the oncolytic herpesvirus for the treatment of melanoma.[19] A series of studies has evaluated the therapeutic effects of oncolytic viruses in ovarian cancer.[20–23] However, most studies are currently heavily focused on the direct or indirect effects of oncolytic viruses on tumor cells themselves, and attention paid to ascites is limited. Moreover, in most studies, human ovarian cancer cell lines were used to evaluate oncolytic effects in immune-

Received 2 April 2021; accepted 7 November 2021;
https://doi.org/10.1016/j.omto.2021.11.008.

Correspondence: Hongxin Deng, PhD, State Key Laboratory of Biotherapy and Cancer Center, Collaborative Innovation Center of Biotherapy, West China Hospital, Sichuan University, Ke-yuan Road 4, No. 1, Gao-peng Street, Chengdu, Sichuan 610041, P.R. China.
E-mail: denghongx@scu.edu.cn

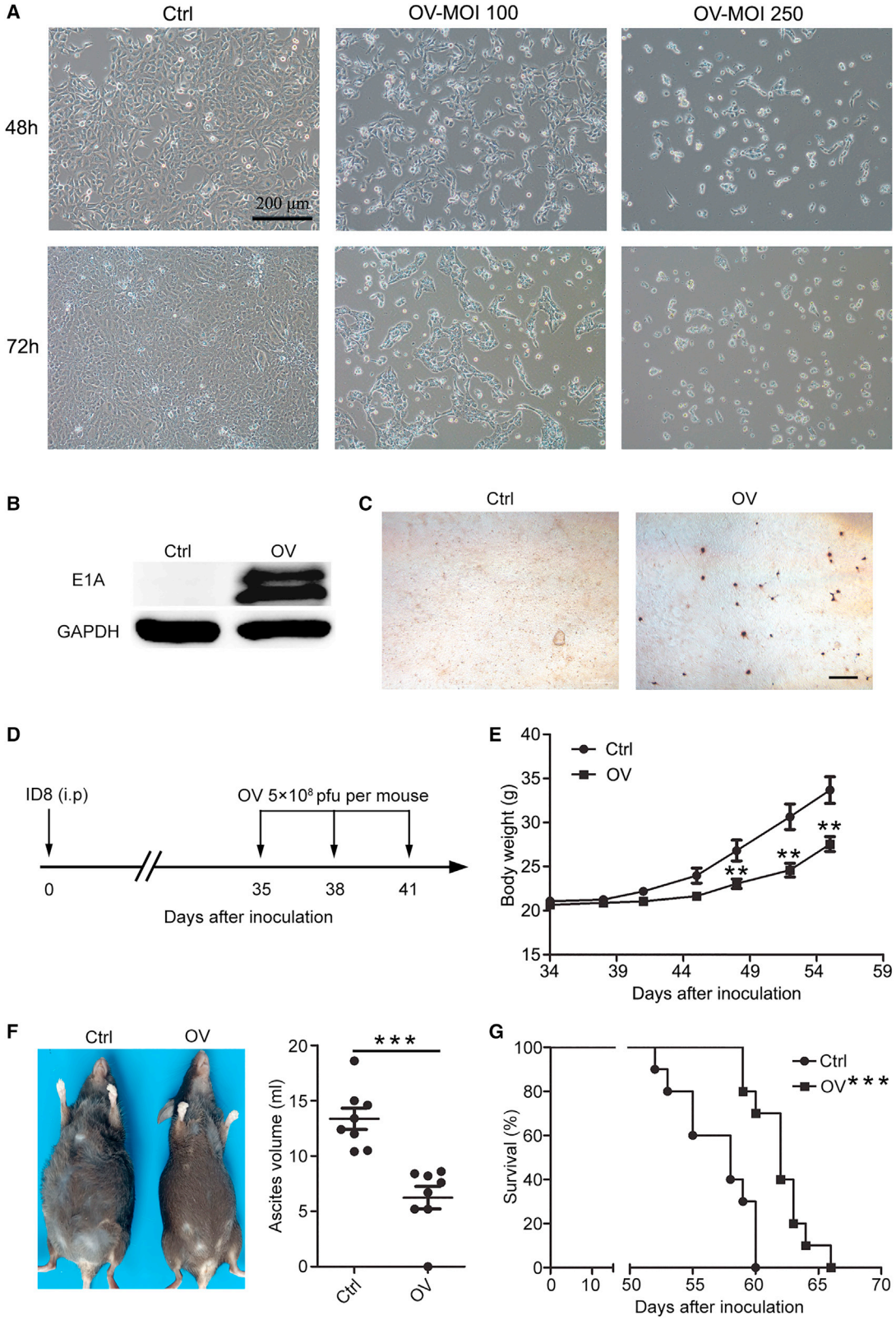

(legend on next page)

deficient mice, which restricted immunological exploration of oncolytic viruses in ascites.

In the present study, we established a mouse ovarian cancer model that mimicked advanced ovarian cancer with ascites formation[24] and investigated the effects of oncolytic adenovirus (OV) on malignant ascites. From our data, we provide an insight into the capacity of OV to control ascites and potential immune mechanisms, which might be helpful for the clinical treatment of patients with advanced ovarian cancer.

RESULTS

OV lysed the mouse ovarian cancer cells and suppressed ascites formation *in vivo*

We first tested the oncolytic effects of OV on mouse ID8 ovarian cancer cells, as shown in Figure 1A. Compared with the control group, OV lysed the ID8 cells and significantly decreased their cell numbers after infection. We also detected the expression of virus-specific gene E1A and progeny virus post infection (Figures 1B and 1C). We then evaluated the effects of OV *in vivo* on the ascites whereby the mice were treated according to the scheme shown in Figure 1D and ascites development was indicated by body weight, with the results showing that OV treatment remarkably arrested the increase of body weight in mice (Figure 1E). Further measurement of ascites volume also suggested that a smaller volume was present in the treated group than in the untreated group (Figure 1F). Moreover, OV treatment prolonged the OS of the mice (Figure 1G). Therefore, these results revealed that OV greatly reduced ascites formation.

OV reshaped the immune cell profile of ascites

Given the above results that reduced ascites volume was observed after OV treatment, we analyzed the infiltrating immune cell profiles within the ascites using flow cytometry and found that OV treatment increased the total number of T cells (Figure 2A). The T cell subset analysis suggested that only $CD8^+$ T cells, but not $CD4^+$ T cells, increased (Figure 2B), which led to an increase in the ratio of $CD8^+$ T cells to $CD4^+$ T cells (Figure 2C). Previous studies indicated that effector T cells in ascites were positively correlated with ovarian cancer progression.[10,12] We next determined the percentage of naive and effector T cells after treatment, which was defined as $CD44^{-/low}CD62L^+$ and $CD44^{high}CD62L^-$, respectively (Figure 2D). We found that the percentage of effector T cells was relatively low in the control group, and most $CD4^+$ T cells were naive. However, OV treatment reversed this effect, resulting in remarkable enhancement of $CD4^+$ effector T cells and decrease of $CD4^+$ naive T cells (Figures 2E and 2F); similar results were also found in the $CD8^+$ T cell subsets (Figures 2G and 2H). We then investigated whether these T cells could target tumor antigens, and the results showed that OV therapy increased the percentage of tumor-specific $CD8^+$ T cells in ascites (Figure 2I).

The role of macrophages in maintaining the immunosuppressive microenvironment and promoting cancer progression has been well studied,[25,26] and CSF-1/CSF-1R signaling is important for macrophage recruitment and polarization.[27,28] We also detected constitutive secretion of CSF-1 by ID8 cells (data not shown) and high expression of CSF-1R on macrophages (Figure 2J). The results showed that OV treatment reduced the proportion of macrophages in ascites (Figure 2K) and upregulated the percentage of proinflammatory M1-like macrophages (Figure 2L), as indicated by major histocompatibility complex II (MHC II) expression. Conversely, the number of M2-like macrophages ($CD11b^+F4/80^+$ MHC II^-) was decreased (Figure 2M). CD206 expression, another marker for M2 macrophages, was also downregulated after treatment (Figure 2M), leading to upregulated ratios of M1 to M2 macrophages (Figure 2N). As a result of these positive changes, the proportion of tumor cells in the ascites was remarkably reduced (Figure 2O). Consistent with the change of immune cell profiles, we also found an increase of proinflammatory cytokines (interferon-γ [IFN-γ], CXCL9, and interleukin-2 [IL-2]) and downregulation of immunosuppressive cytokine IL-6 (Figure 2P).

Taken together, OV treatment changed the immune balance by promoting T cell infiltration and differentiation into effector T cells and polarized macrophages toward the M1-like phenotype, which was beneficial for antitumor immunity and disease control.

OV activated T cell function and increased IFN-γ secretion

Based on the key role of T cells in immune-mediated tumor control and the finding that OV enhanced T cell numbers and the percentage of effector T cells in ascites (Figures 2A–2I), we investigated whether the functional level of T cells was also improved. By detecting the expression of the co-stimulatory molecule ICOS on T cells, we found that OV treatment significantly augmented ICOS expression on both the $CD4^+$ and $CD8^+$ T cells of ascites (Figures 3A and 3B), suggesting a stronger activation of T cells after treatment. Proliferation rates are also considered essential indicator of T cell function; here, we found that OV treatment upregulated Ki-67 expression in ascitic $CD4^+$ and $CD8^+$ T cells (Figures 3C and 3D). Notably, despite the fact that the $CD4^+$ T cell number in ascites was not extended after treatment (Figure 2B), both ICOS and Ki-67 expression increased substantially.

To further understand T cell functions, we determined the IFN-γ expression in the T cells from ascites and the spleen and found that, after stimulation with phorbol myristate acetate and ionomycin, the amount of IFN-γ-expressing $CD4^+$ and $CD8^+$ T cells in untreated ascites was low (Figure 3E), suggesting that these T cells were not activated or suppressed by inhibitory signaling; this was consistent with previous results that the IFN-γ in untreated ascites was not detectable (Figure 2P). However, OV treatment largely expanded IFN-γ-expressing T cells,

Figure 1. The oncolytic effects of OV *in vitro* and therapeutic ability *in vivo*

(A) ID8 cell morphology after infection. Scale bar, 200 μm. (B) Expression of adenovirus gene E1A in ID8 cells after infection. (C) Detection of progeny OV in tumor cells after infection. Scale bar, 100 μm. (D) Treatment scheme. (E) Body weights of mice, n = 10 mice per group. (F) Representative mice with ascites and statistics of ascites volume, n = 8 mice per group. (G) Overall survival, n = 10 mice per group. Mean ± SEM is shown. *$p < 0.05$, **$p < 0.01$, ***$p < 0.001$.

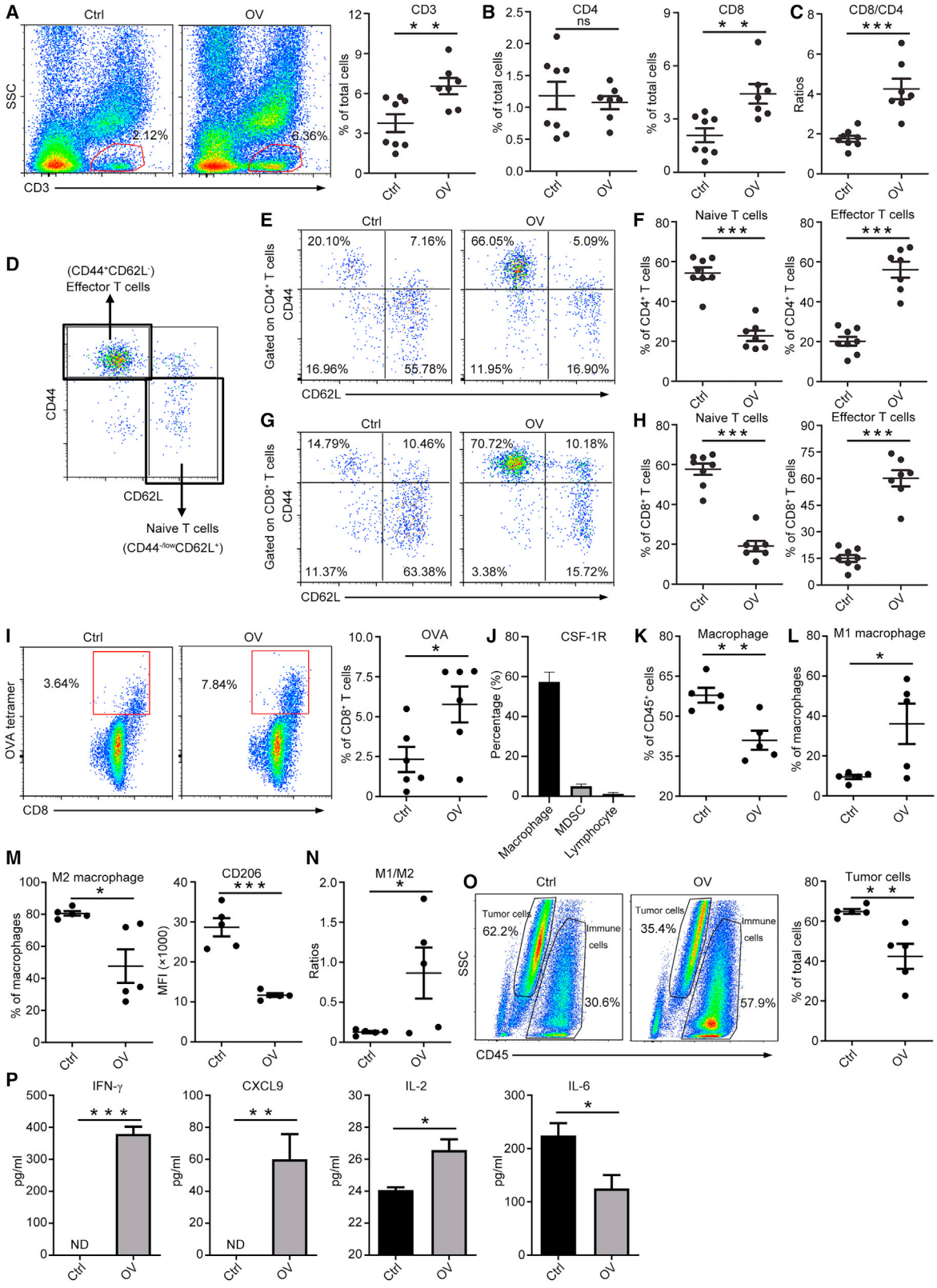

(legend on next page)

especially $CD8^+$ T cells (Figures 3E and 3F). We also detected IFN-γ expression in splenic T cells in response to stimulation; although no significant variation was observed, they did demonstrate a growing trend (Figure 3G).

Therefore, these data provide strong evidence that OV alters ascitic T cell function by enhancing T cell activation, proliferation, and IFN-γ release, which resulted in immune activation and reduced ascites.

OV treatment upregulated the co-inhibitory molecules and increased Treg infiltration

To investigate the immunosuppressive status of ascites after treatment, we initially performed an analysis of co-inhibitory molecules in the ascitic microenvironment, including PD-1/PD-L1 signaling and LAG-3. The results indicated that OV treatment largely augmented PD-1 expression on both ascitic $CD4^+$ and $CD8^+$ T cells (Figures 4A and 4B), suggesting that not only functional activation but also suppressive signaling was enhanced after treatment. OV treatment significantly increased LAG-3 expression on $CD4^+$ T cells (Figure 4C). It was noteworthy that the overall percentage of LAG-3 on $CD4^+$ T cells was low (<15%); however, the increased amount of LAG-3 was more significant in $CD8^+$ T cells than in $CD4^+$ T cells (Figure 4D). As a consequence, the number of $PD\text{-}1^+LAG\text{-}3^+$ double-positive $CD4^+$ T cells and $CD8^+$ T cells, which indicated a severely exhausted status,[29] was increased (Figure 4E). We then determined PD-L1 expression on ascitic tumor cells, total immune cells, and macrophages. The results showed that OV treatment led to a tremendous increase of PD-L1 abundance on ascitic tumor cells (Figure 4F). Although the percentage of PD-L1 expression on total immune cells was not altered after treatment (Figure 4G), PD-L1 expression on macrophages was significantly upregulated, with an average of nearly 100% (Figure 4H), which was in line with the fact that inhibitory signals constitutively existed or were induced in ascites.[4] Finally, we evaluated the proportion of regulatory T cells (Tregs), which are closely associated with cancer development and immune suppression,[30] and found that OV treatment led to a remarkable increase in Tregs (Figure 4I).

In brief, despite OV treatment boosting T cell infiltration and activation, it also induced immune-suppressive mechanisms by upregulating the expression of co-inhibitory molecules and enhancing immune-suppressive cell infiltration.

Combination therapy with OV, PLX3397, and anti-PD-1 restrained ascites development

Inspired by the finding that OV treatment enhanced PD-1 expression on T cells and due to the advantages of combination therapy in overcoming multiple suppressive factors, we also found that CSF-1R was mainly expressed on macrophages (Figure 2J), CSF-1/CSF-1R is a key signal pathway for macrophage recruitment.[31,32] Therefore, we designed a triple combination strategy that included OV, PD-1 antibodies, and PLX3397 (a CSF-1R inhibitor) and tested its potential disease control abilities. The results suggested that, compared with monotherapy and dual therapy, mice that received combination therapy had greatly delayed increase of body weight (Figures 5A and 5B). These data suggest that combination therapy can induce strong therapeutic effects on ascites formation.

Combination therapy increased T cell infiltration and altered macrophage polarization

We next wanted to uncover the possible mechanism behind combination therapy. Thus, an analysis of T cells and macrophages in ascites was performed using flow cytometry. The ascites volume was measured before immune cell analysis, and the results indicated that the combined group had a smaller volume of ascites than the untreated group (Figure 5C). The data from analysis of immune cell profiles showed that combination treatment significantly expanded T cell infiltration (Figure 5D) as well as the percentage of $CD4^+$ and $CD8^+$ T cells (Figure 5E). Increased ratios of $CD8^+$ T cells to $CD4^+$ T cells were also achieved after combination therapy (Figure 5F). Although an enhancement of Tregs was observed, the immunosuppressive microenvironment was reversed, as suggested by the increased ratios of activated $CD8^+$ T cells ($CD8^+ICOS^+$) to Tregs after combination therapy (Figure 5G). We then determined the percentage of macrophages. It was interesting that combination therapy did not affect their proportion (Figure 5H); however, combination treatment remarkably altered their phenotypes, which improved the percentage of M1 phenotypes (Figures 5I and 5J) and reduced M2 macrophages (Figures 5K and 5L), leading to an increased ratio of M1 to M2 macrophages (Figure 5M). In summary, combination therapy resulted in an extension of T cells and polarization of macrophages.

Combination treatment promoted T cell proliferation and activation

Having confirmed increased T cell infiltration, we next tried to obtain an overall understanding of the T cells in ascites after combination

Figure 2. OV changes the immune cell profiles in ascites

(A) Percentage of total T cells in ascites; representative flow data and statistics are shown, n = 7–8 mice per group. (B) Percentage of $CD4^+$ and $CD8^+$ T cells in ascites, n = 7–8 mice per group. (C) Ratios of $CD8^+$ T cells to $CD4^+$ T cells in ascites, n = 7–8 mice per group. (D) Gating strategy for effector T cell ($CD44^+CD62L^-$) and naive T cell ($CD44^{-/low}CD62L^+$) in ascites. (E and F) Proportion of $CD4^+$ effector T cells and naive T cells in ascites; representative flow data (E) and statistics (F) are shown, n = 7–8 mice per group. (G and H) Percentage of $CD8^+$ effector T cells and naive T cells in ascites; representative flow data (G) and statistics (H) are shown, n = 7–8 mice per group. (I) Percentage of antigen-specific $CD8^+$ T cells in ascites, n = 6 mice per group. (J) CSF-1R expression on macrophages, MDSCs, and lymphocytes in ascites, n = 3 mice. (K) Percentage of macrophages ($CD11b^+F4/80^+$) in ascites, gated on $CD45^+$ cells, n = 5 mice per group. (L) Proportion of M1 macrophages in ascites, identified as MHC II expression, gated on $CD11b^+F4/80^+$, n = 5 mice per group. (M) Ratio of M2 macrophages ($CD11b^+F4/80^+$ MHC II^-) and the CD206 expression on macrophages, n = 5 mice per group. (N) Ratios of M1 to M2 macrophages, n = 5 mice per group. (O) Proportion of tumor cells ($CD45^-$ cells) in ascites, n = 5 mice per group. (P) Concentration of inflammatory cytokines in ascites, n = 4 mice per group. ND, not detectable. Mean ± SEM is shown. *p < 0.05, **p < 0.01, ***p < 0.001; ns, no statistical significance.

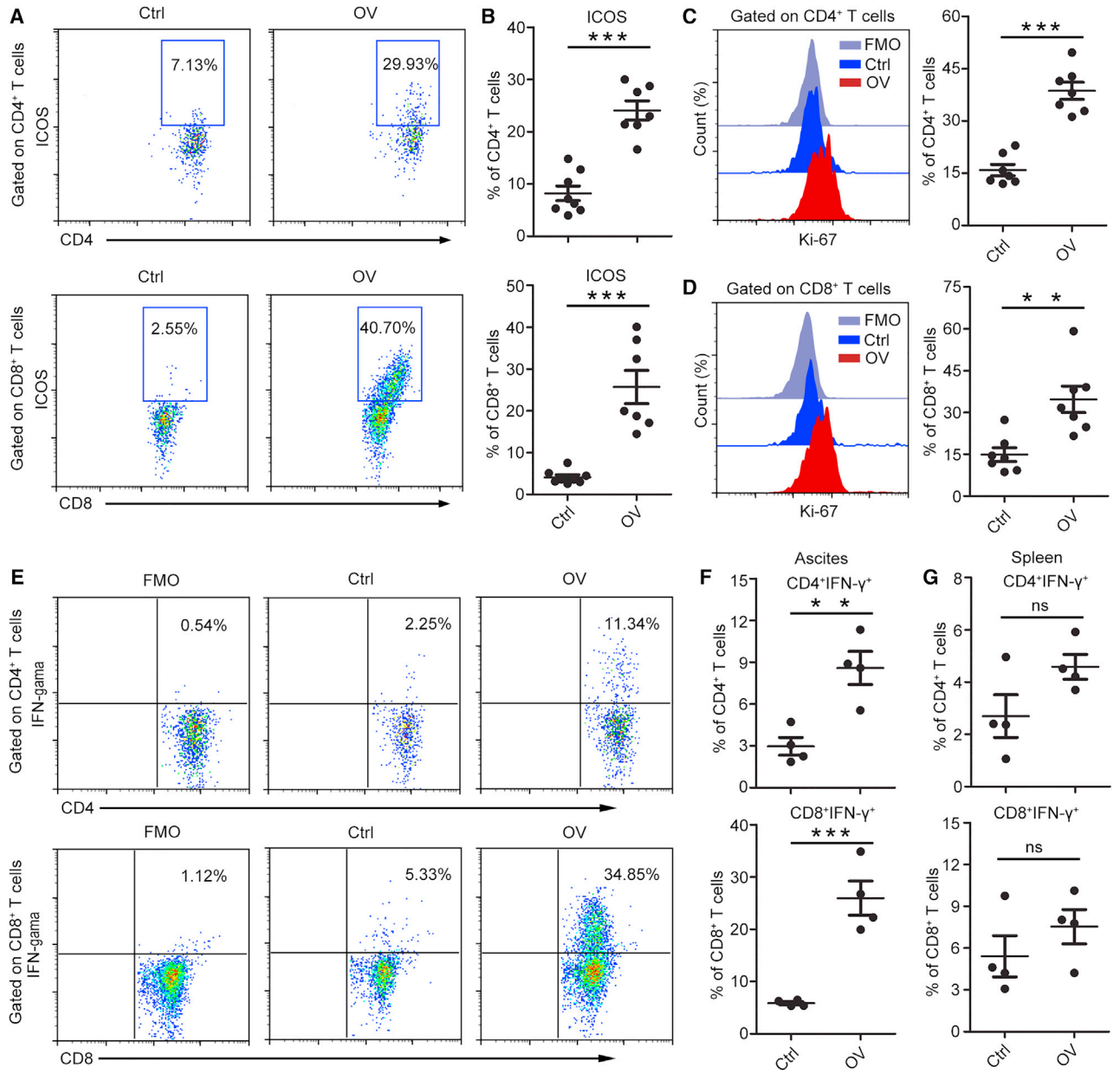

Figure 3. T cell activation after OV treatment

(A and B) Expression of ICOS on $CD4^+$ T and $CD8^+$ T cells in ascites; representative flow data (A) and statistics (B) are shown, n = 7–8 mice per group. (C) Ki-67 expression in $CD4^+$ T cells, n = 7–8 mice per group. (D) Ki-67 expression in ascitic $CD8^+$ T cells, n = 7–8 mice per group. (E) Percentage of IFN-γ-expressing $CD4^+$ and $CD8^+$ T cells in ascites. (F) Statistics for IFN-γ-expressing $CD4^+$ and $CD8^+$ T cells in ascites, n = 4 mice per group. (G) Statistics for IFN-γ-expressing $CD4^+$ and $CD8^+$ T cells in spleen, n = 4 mice per group. Mean ± SEM is shown. *p < 0.05, **p < 0.01, ***p < 0.001; ns, no statistical significance.

therapy. We initially detected their differentiated status with treatment and found that combination treatment promoted T cell differentiation from naive T cell to effector T cells, which resulted in an increase of effector T cells and reduction of naive T cells in $CD4^+$ T cells (Figures 6A and 6B) and $CD8^+$ T cells (Figures 6C and 6D). We speculated that this differentiation was driven by OV, since previous results from OV treatment showed the same effects (Figure 2). Moreover, as suggested by the upregulated expression of the co-stimulatory molecule ICOS on the T cell surface, we also found enhanced activation of $CD4^+$ T cells (Figure 6E) and $CD8^+$ T cells (Figure 6F). Finally, we evaluated the proliferation ability of T cells via the detection of Ki-67 expression, which is a prerequisite for their augmentation and function. In $CD4^+$ T cells, combination treatment dramatically upregulated Ki-67 expression (Figure 6G), and similar results were also

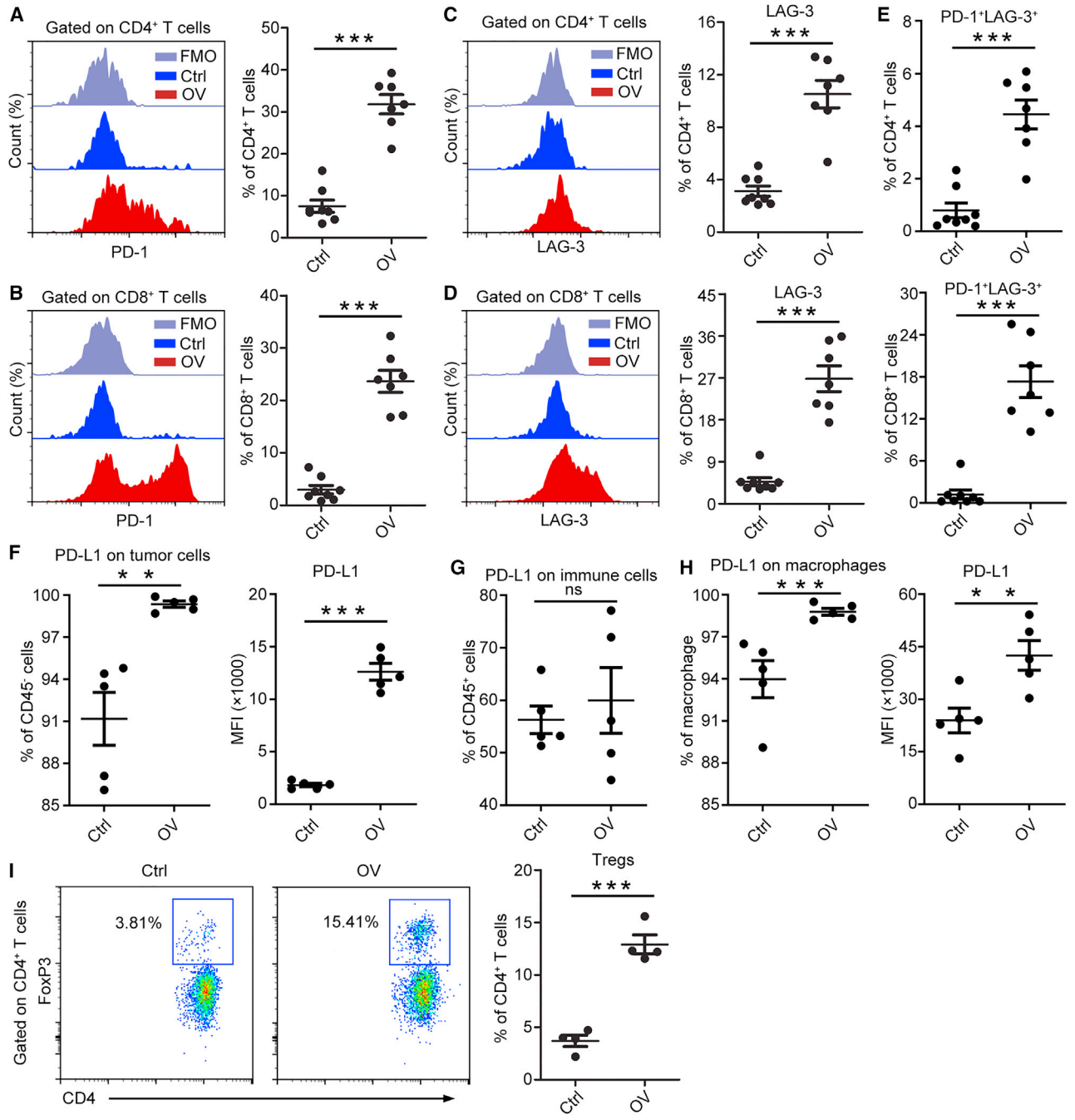

Figure 4. Detection of immunosuppressive factors in ascites

(A and B) PD-1 expression on ascitic CD4$^+$ and CD8$^+$ T cells; representative flow data and statistics are shown, n = 7–8 mice per group. (C and D) LAG-3 expression on CD4$^+$ and CD8$^+$ T cells in ascites; representative flow data and statistics are shown, n = 7–8 mice per group. (E) Percentage of PD-1$^+$LAG-3$^+$ T cells, n = 7–8 mice per group. (F) PD-L1 expression on ascitic tumor cells (CD45$^-$ cells), n = 5 mice per group. (G) Proportion of PD-L1 expression on immune cells, n = 5 mice per group. (H) Proportion of PD-L1 expression on macrophages, n = 5 mice per group. (I) Percentage of Tregs in ascites; representative flow data and statistics are shown, n = 4 mice per group. Mean ± SEM is shown. *p < 0.05, **p < 0.01, ***p < 0.001; ns, no statistical significance.

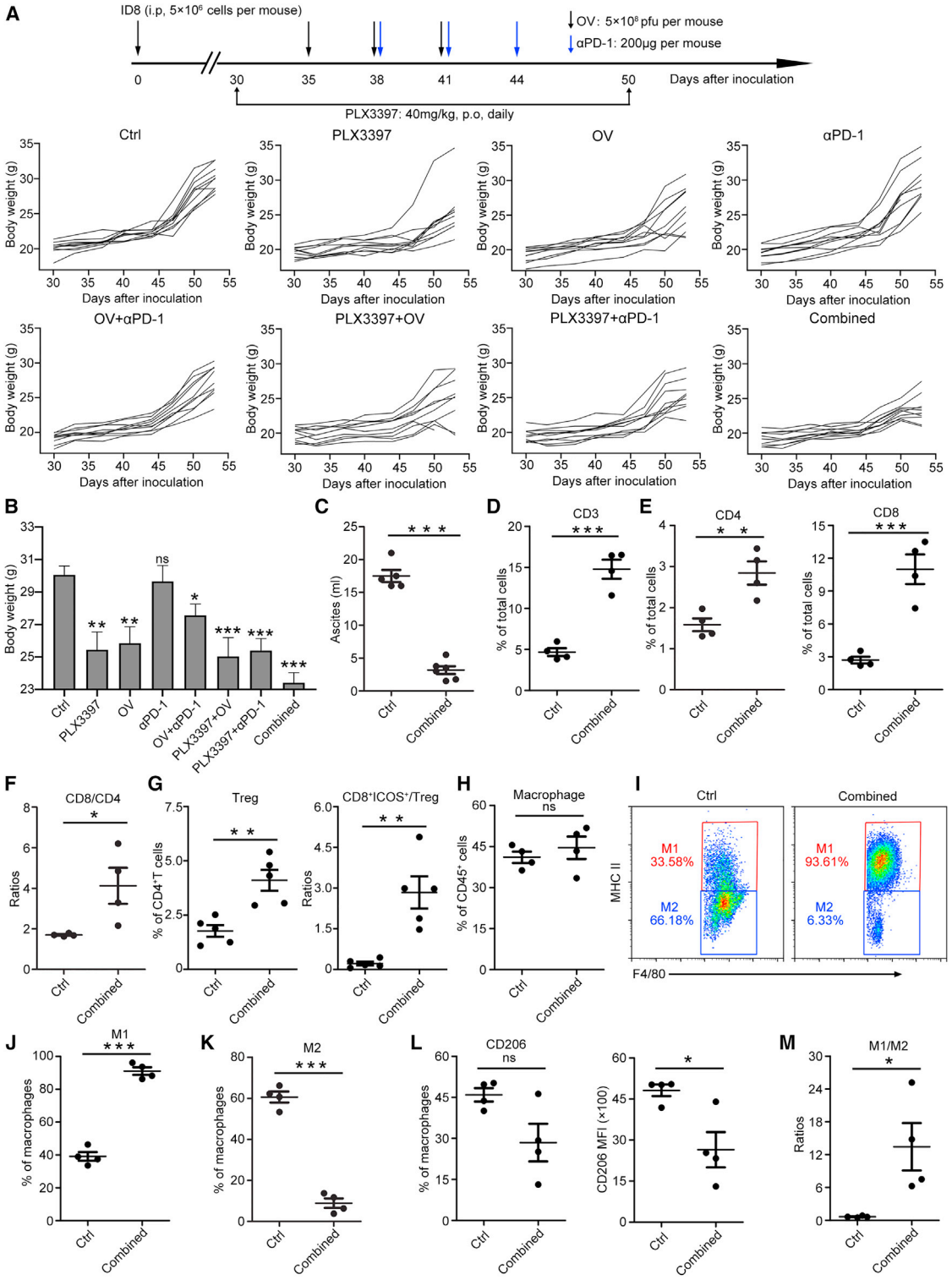

Figure 5. Therapeutic effects and immune cell changes in ascites after combination therapy

(A) Combination treatment scheme and individual body growth of mice, n = 10 mice per group. (B) Body weight on days 53, n = 10 mice per group. (C) Ascites volume, n = 5 mice per group. (D) Proportion of total T cells ($CD3^+$) in ascites, n = 4 mice per group. (E) Percentage of ascitic $CD4^+$ and $CD8^+$ T cells, n = 4 mice per group. (F) Ratios of $CD8^+$ T cells to $CD4^+$ T cells, n = 4 mice per group. (G) Percentage of Tregs in ascites and the ratios of activated $CD8^+$ T cells to Tregs, n = 5 mice per group. (H) Percentage of

(legend continued on next page)

achieved in $CD8^+$ T cells, with more than 80% of $CD8^+$ T cells showing positive signals (Figure 6H). Consequently, combination therapy significantly promoted T cell activation and proliferation in ascites.

DISCUSSION

Recent studies have indicated that malignant ascites are important indicators of poor prognosis and are promotive factors of ovarian cancer.[33] Therefore, the management of ascites is an essential part of effective therapy for ovarian cancer. Unexpectedly, most efforts are being made to explore treatments that target the tumor cells themselves. To date, treatments or evaluations that focus on ascites are less investigated. Catumaxomab, a trifunctional monoclonal antibody, was approved for intraperitoneal therapy of malignant ascites in the European Union in 2009.[34,35] It can target CD3 on T cells and epithelial cell-adhesion molecule expressed on most epithelial cancers, and can induce antibody-dependent cell-mediated cytotoxicity via the Fc-γ receptor. Anti-angiogenic therapy is another potential strategy for the treatment of malignant ascites, considering that VEGF is consistently detected in ascites and enhances the permeability of the endothelium. Several studies have reported the clinical benefits of targeting VEGF with bevacizumab in ovarian cancer cases.[36,37] However, the possible benefits of ascites control have not yet been reported. In the present study, we found that OV could remarkably control ascites development by reprogramming the ascitic immune microenvironment toward proinflammatory status; in particular, OV treatment increased T cell infiltration, activation, and function, especially in $CD8^+$ T cells, while OV also promoted T cell differentiation from naive T cells to effector T cells.

Oncolytic viruses have shown great potential in the field of cancer therapy,[38,39] while the use of oncolytic viruses has led to tremendous success in preclinical and clinical research and was approved by the US Food and Drug Administration for the treatment of melanoma in 2015.[19,40] Despite the many attractive features of oncolytic virotherapy, it is generally believed that local or intratumoral administration is one of the major factors that limit the extensive application of oncolytic viruses, due to their lack of tumor-targeting abilities and the pre-existing antiviral immunity of patients. This makes local administration, which is a suboptimal delivery compared with systemic injection, as a preferred choice in clinical treatment. Moreover, due to their location, most tumors are difficult to treat locally. In view of this, ascites provide a favorable platform from which oncolytic virotherapy can overcome this delivery deficiency and achieve several benefits, one of these being that intraperitoneal injection makes metastatic tumor cells more accessible to oncolytic viruses and facilitates direct tumor killing. Another benefit is the remodeling effects of oncolytic viruses on the ascitic immune microenvironment, which can further improve the therapeutic efficacy, as abundant tumor-promoting factors accumulate in ascites and can contribute to tumor cell metastasis.[26,41] The effects of oncolytic virus on a mouse ID8 ovarian cancer model have been reported by several studies;[42–44] however, most of their efforts were focused on the direct effects of virus on cancer cells rather than ascites. The present study, although only one cancer model was used due to the lack of a mouse model of ovarian cancer, provided insights into ascitic immune cell profiles and rates of disease control following OV treatment, whereby OV treatment reversed the immune balance by promoting T cell activation and differentiation from the naive phenotype into the effector phenotype. It also reprogrammed anti-inflammatory M2 macrophages toward the proinflammatory M1 phenotype, which significantly delayed the development of ascites. These findings were in line with previous reports that ascites with an immunoreactive phenotype and higher ratio of CD8/CD4 predicted a good prognosis.[11,12]

Multifactorial pathogenesis and resistance mechanisms induced after treatment are major factors that attenuate the effects of monotherapy.[45–47] In the present study, PD-L1 was highly expressed on both the tumor cells and immune cells in the ascitic microenvironment, as well as on a high percentage of macrophages, most of which were the tumor-promoting M2 phenotype. Notably, OV treatment enhanced the expression of co-inhibitory molecules PD-1 and LAG-3 on T cells, suggesting an exhausted status of the T cells in ascites. Moreover, OV treatment significantly increased Treg infiltration. These data indicate the emergence of immunosuppressive mechanisms triggered by OV treatment. In this context, numerous preclinical and clinical studies have shown that combination therapy is an ideal approach to overcome one or more resistant mechanisms and to improve outcomes.[18,48,49] Based on pre-existent and inducible inhibitory molecules and cells, we tested a combination strategy that included OV, PLX3397, and anti-PD-1, which was reported in our previous study to confer effective antitumor abilities in mouse colon cancer.[50] Combination therapy also remarkably reduced the ascites burden. Furthermore, combination treatment generated more effective ICOS and Ki-67 expression, suggesting stronger T cell activation and function. Results from other studies also showed that upregulation of co-inhibitory molecules such as PD-1, LAG-3, and CTLA-4 could dampen antitumor immunity in ovarian cancer, and dual blockade of LAG-3 and PD-1 restrained tumor growth in mouse ovarian cancer.[51,52] The immune-regulatory ability of oncolytic viruses may provide a rational basis for combination therapy of metastatic ovarian cancer with peritoneal metastasis.

In summary, our study demonstrates the potential therapeutic effects of oncolytic viruses on ovarian cancer-associated malignant ascites by reprogramming the ascitic immune microenvironment, as well as making virotherapy a potential candidate for the treatment of advanced ovarian cancer by targeting both cancer cells and ascites.

macrophages, n = 4 mice per group. (I) Gating strategy for M1 and M2 macrophages in ascites. (J) Proportion of M1 macrophages, n = 4 mice per group. (K) Proportion of M2 macrophages, n = 4 mice per group. (L) CD206 expression; the percentage and mean fluorescence intensity are shown, n = 4 mice per group. (M) Ratios of M1 to M2 macrophages, n = 4 mice per group. Mean ± SEM is shown. *$p < 0.05$, **$p < 0.01$, ***$p < 0.001$; ns, no statistical significance.

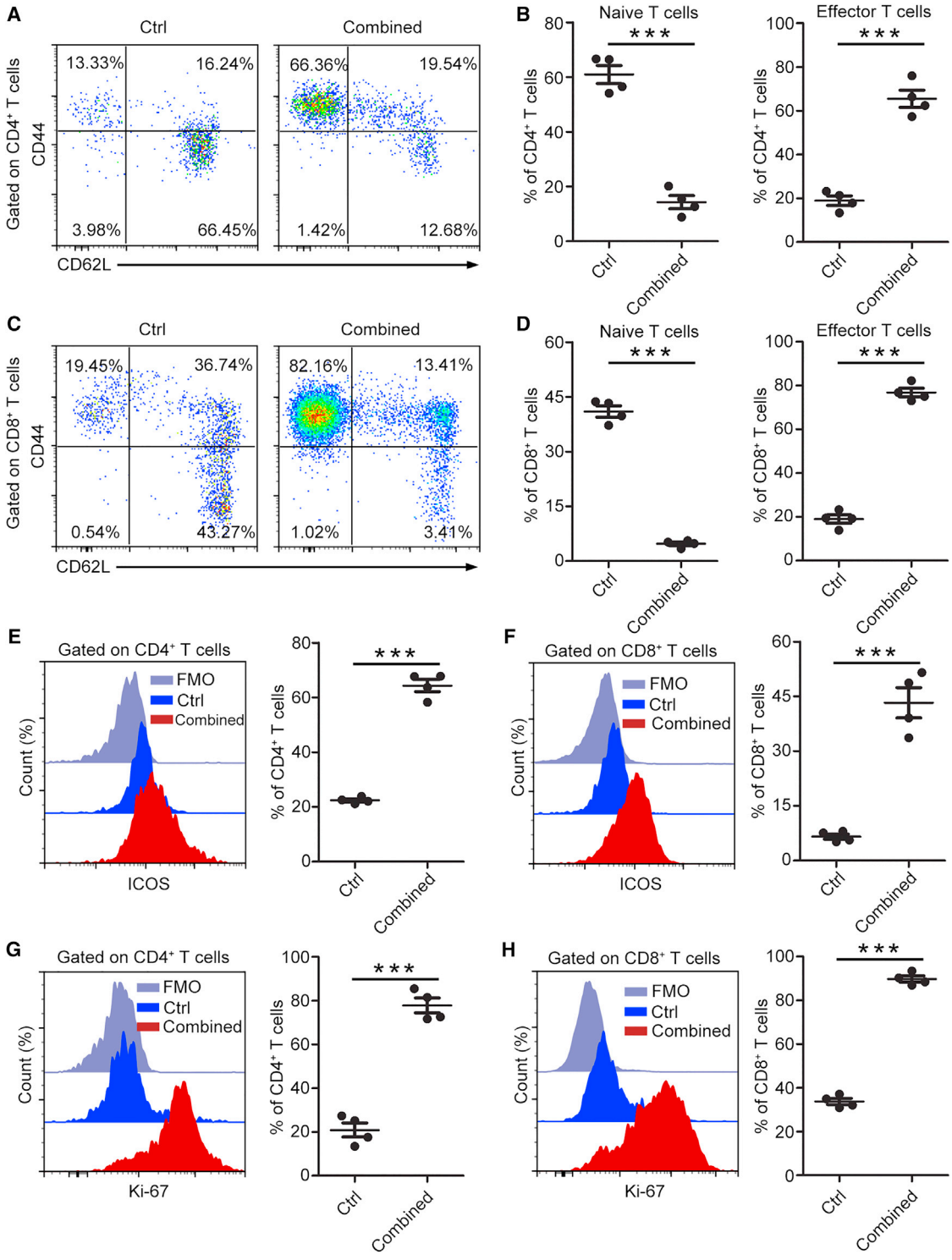

Figure 6. Immune activation effects in ascites after combination therapy

(A and B) Proportion of CD4$^+$ effector T cells (CD44$^+$CD62L$^-$) and naive T cells (CD44$^{-/low}$CD62L$^+$) in ascites; representative flow data (A) and statistics (B) are shown, n = 4 mice per group. (C and D) Proportion of CD8$^+$ effector T cells (CD44$^+$CD62L$^-$) and naive T cells (CD44$^{-/low}$CD62L$^+$) in ascites; representative flow data (C) and statistics (D) are shown, n = 4 mice per group. (E) ICOS expression on ascitic CD4$^+$ T cells, n = 4 mice per group. (F) ICOS expression on ascitic CD8$^+$ T cells, n = 4 mice per group. (G) Ki-67 expression in ascitic CD4$^+$ T cells, n = 4 mice per group. (H) Ki-67 expression in ascitic CD8$^+$ T cells, n = 4 mice per group. Mean ± SEM is shown. *p < 0.05, **p < 0.01, ***p < 0.001.

MATERIALS AND METHODS

Mice and cell line

Six-to eight-week-old C57BL/6 female mice were purchased from Beijing Huafukang Bioscience (Beijing, China). The mouse ovarian cancer line ID8[24] and ID8-OVA were kindly obtained from Professor Xia Zhao (West China Second Hospital, Sichuan University, Chengdu, China) and were supplemented in Dulbecco's modified Eagle's medium (DMEM; Gibco) with 10% fetal bovine serum (FBS; Gibco), and were maintained at 37°C and 5% CO_2 in an incubator.

Viruses and antibodies

Oncolytic adenovirus (OV) is a type 5 adenovirus with depleted E1b and E3 genes and a retained E1a gene. The human telomerase reverse transcriptase promoter was inserted upstream of the E1A gene to control virus replication. The OV was packaged and amplified in 293T cells, and ultracentrifugation was used for purification. Therapeutic anti-PD-1 antibodies were provided by Innovent Biologics (Suzhou, Jiangsu, China). Fluorescence-labeling antibodies to CD3 (17A2), CD4 (RM4-5), CD45 (30-F11), CD11b (M1/70), F4/80 (BM8), CD206 (C068C2), LAG-3 (C9B7W), PD-1 (RMP1-30), ICOS (7E.17G9), CD44 (IM7), CD62L (MEL-14), MHCII (M5/114.15.2), and Ki67 (16A8) were purchased from BioLegend, and antibodies to CD8 (53-6.7), FoxP3 (MF23), and IFN-γ (XMG1.2) were purchased from BD Bioscience. Antibody to adenovirus-5 E1A was purchased from Santa Cruz Biotechnology. OVA Tetramer-SIINFEKL-PE and fluorescein isothiocyanate-labeling anti-CD8 (KT15) were purchased from MBL.

Detection of progeny adenovirus in tumor cells

ID8 cells were infected with OV (MOI: 100) for 2 h, and the supernatant was replaced with fresh DMEM (5% FBS). After incubation for 72 h, cells and supernatant were collected and freeze-thawed three times, then the supernatant was collected after centrifugation and diluted 1,000-fold. The OV titer was determined using the Adeno-XTM Rapid Titer Kit (TaKaRa). In brief, HEK 293 cells (2.5×10^5 cells per well) and 50 μL of diluted supernatant were seeded into a 24-well plate and cultured for 48 h. The cells were fixed and stained according to the manufacturer's instructions.

Tumor model and treatment

Tumor cells (5×10^6) were intraperitoneally injected in 500 μL of serum-free medium, and ascites development was monitored by measuring body weight twice a week. OV (5×10^8 plaque-forming units [PFU] per mouse) was administered intraperitoneally (i.p.) on days 35, 38, and 41 after inoculation. For combination therapy, PLX3397 treatment (40 mg/kg, Selleck) was administered daily from day 30 to day 50 after inoculation by gavage. OV (i.p., 5×10^8 PFU per mouse) was injected on days 35, 38, and 41, and anti-PD-1 (i.p., 200 μg per mouse) was administered on days 38, 41, and 44 after inoculation. Mice that succumbed to ascites and tumors were recorded for OS statistics, and animal experiments were performed in accordance with the Animal Care and Use Committee of West China Hospital, Sichuan University, China.

Flow cytometry

Mice were sacrificed on day 5 after last OV (monotherapy) or anti-PD-1 (combination therapy) injection, ascites was collected for volume measurement, and the cells were collected for flow cytometry, blocked with anti-mouse CD16/CD32 (Fc block, BD Bioscience) and stained with fluorescence-labeling antibodies at 4°C for 30 min. For intracellular staining, cell surface markers were stained, then cells were permeabilized with a FoxP3 fixation and permeabilization kit (eBioscience) for Ki-67 staining or with a Fixation/Permeabilization Kit (BD Bioscience) for IFN-γ staining. Cells used for IFN-γ staining were pretreated with Leukocyte Activation Cocktail containing Brefeldin A (BD Bioscience). In some analyses, fluorescence-minus-one was used to identify positive signals.

Statistical analysis

Data were analyzed using GraphPad Prism version 5. Statistical significance was analyzed using an unpaired t test. OS was presented using Kaplan-Meier survival curves and analyzed using the log-rank test. Differences were considered statistically significant at $p < 0.05$. Asterisks were used to denote $^*p < 0.05$, $^{**}p < 0.01$, $^{***}p < 0.001$; "ns" denotes no statistical significance.

ACKNOWLEDGMENTS

This research was supported by the Fundamental Research Funds for the Central Universities (2020SCU12024), 1.3.5 project for disciplines of excellence, West China Hospital, Sichuan University (ZYGD20003), and the National Natural Science Foundation of China Program grant 81902918.

AUTHOR CONTRIBUTIONS

G.S. and H.D. were involved in obtaining funding and study supervision; P.S., Y.Y., and Z.D. performed all the animal experiments; J.X. and L.S. were involved in the acquisition and analysis of the flow data; J.M. and P.C. were involved in virus amplification and purification; L.D., Y.Z., and L.C. provided advice in study design and interpretation of data.

DECLARATION OF INTERESTS

The authors declare no competing interests.

REFERENCES

1. Ahmed, N., and Stenvers, K.L. (2013). Getting to know ovarian cancer ascites: opportunities for targeted therapy-based translational research. Front. Oncol. *3*, 256.

2. Krugmann, J., Schwarz, C.L., Melcher, B., Sterlacci, W., Ozalinskaite, A., Lermann, J., Agaimy, A., and Vieth, M. (2019). Malignant ascites occurs most often in patients with high-grade serous papillary ovarian cancer at initial diagnosis: a retrospective analysis of 191 women treated at Bayreuth Hospital, 2006-2015. Arch. Gynecol. Obstet. *299*, 515–523.

3. Cavazzoni, E., Bugiantella, W., Graziosi, L., Franceschini, M.S., and Donini, A. (2013). Malignant ascites: pathophysiology and treatment. Int. J. Clin. Oncol. *18*, 1–9.

4. Ford, C.E., Werner, B., Hacker, N.F., and Warton, K. (2020). The untapped potential of ascites in ovarian cancer research and treatment. Br. J. Cancer *123*, 9–16.

5. Hodge, C., and Badgwell, B.D. (2019). Palliation of malignant ascites. J. Surg. Oncol. *120*, 67–73.

6. Kipps, E., Tan, D.S., and Kaye, S.B. (2013). Meeting the challenge of ascites in ovarian cancer: new avenues for therapy and research. Nat. Rev. Cancer *13*, 273–282.
7. Szender, J.B., Emmons, T., Belliotti, S., Dickson, D., Khan, A., Morrell, K., Khan, A., Singel, K.L., Mayor, P.C., Moysich, K.B., et al. (2017). Impact of ascites volume on clinical outcomes in ovarian cancer: a cohort study. Gynecol. Oncol. *146*, 491–497.
8. Huang, H., Li, Y.J., Lan, C.Y., Huang, Q.D., Feng, Y.L., Huang, Y.W., and Liu, J.H. (2013). Clinical significance of ascites in epithelial ovarian cancer. Neoplasma *60*, 546–552.
9. Lai, I., Daniel, M.N., Rosen, B.P., May, T., Massey, C., and Feigenberg, T. (2019). Correlation of differential ascites volume with primary cytoreductive surgery outcome, lymph node involvement, and disease recurrence in advanced ovarian cancer. Int. J. Gynecol. Cancer *29*, 922–928.
10. Feigenberg, T., Clarke, B., Virtanen, C., Plotkin, A., Letarte, M., Rosen, B., Bernardini, M.Q., Kollara, A., Brown, T.J., and Murphy, K.J. (2014). Molecular profiling and clinical outcome of high-grade serous ovarian cancer presenting with low- versus high-volume ascites. Biomed. Res. Int. *2014*, 367103.
11. Giuntoli, R.L., 2nd, Webb, T.J., Zoso, A., Rogers, O., Diaz-Montes, T.P., Bristow, R.E., and Oelke, M. (2009). Ovarian cancer-associated ascites demonstrates altered immune environment: implications for antitumor immunity. Anticancer Res. *29*, 2875–2884.
12. Lieber, S., Reinartz, S., Raifer, H., Finkernagel, F., Dreyer, T., Bronger, H., Jansen, J.M., Wagner, U., Worzfeld, T., Müller, R., et al. (2018). Prognosis of ovarian cancer is associated with effector memory CD8(+) T cell accumulation in ascites, CXCL9 levels and activation-triggered signal transduction in T cells. Oncoimmunology *7*, e1424672.
13. Harrington, K., Freeman, D.J., Kelly, B., Harper, J., and Soria, J.C. (2019). Optimizing oncolytic virotherapy in cancer treatment. Nat. Rev. Drug Discov. *18*, 689–706.
14. Zhang, B., and Cheng, P. (2020). Improving antitumor efficacy via combinatorial regimens of oncolytic virotherapy. Mol. Cancer *19*, 158.
15. Ma, X.Y., Hill, B.D., Hoang, T., and Wen, F. (2021). Virus-inspired strategies for cancer therapy. Semin. Cancer Biol. https://doi.org/10.1016/j.semcancer.2021.06.021.
16. Russell, S.J., and Barber, G.N. (2018). Oncolytic viruses as antigen-agnostic cancer vaccines. Cancer Cell *33*, 599–605.
17. Zamarin, D., Holmgaard, R.B., Subudhi, S.K., Park, J.S., Mansour, M., Palese, P., Merghoub, T., Wolchok, J.D., and Allison, J.P. (2014). Localized oncolytic virotherapy overcomes systemic tumor resistance to immune checkpoint blockade immunotherapy. Sci. Transl. Med. *6*, 226ra232.
18. Galon, J., and Bruni, D. (2019). Approaches to treat immune hot, altered and cold tumours with combination immunotherapies. Nat. Rev. Drug Discov. *18*, 197–218.
19. Ledford, H. (2015). Cancer-fighting viruses win approval. Nature *526*, 622–623.
20. Hoare, J., Campbell, N., and Carapuça, E. (2018). Oncolytic virus immunotherapies in ovarian cancer: moving beyond adenoviruses. Porto Biomed. J. *3*, e7.
21. Leung, E.Y.L., Ennis, D.P., Kennedy, P.R., Hansell, C., Dowson, S., Farquharson, M., Spiliopoulou, P., Nautiyal, J., McNamara, S., Carlin, L.M., et al. (2020). NK cells augment oncolytic adenovirus cytotoxicity in ovarian cancer. Mol. Ther. Oncolytics *16*, 289–301.
22. Santos, J.M., Heiniö, C., Cervera-Carrascon, V., Quixabeira, D.C.A., Siurala, M., Havunen, R., Butzow, R., Zafar, S., de Gruijl, T., Lassus, H., et al. (2020). Oncolytic adenovirus shapes the ovarian tumor microenvironment for potent tumor-infiltrating lymphocyte tumor reactivity. J. Immunother. Cancer *8*, e000188.
23. Matuszewska, K., Santry, L.A., van Vloten, J.P., AuYeung, A.W.K., Major, P.P., Lawler, J., Wootton, S.K., Bridle, B.W., and Petrik, J. (2019). Combining vascular normalization with an oncolytic virus enhances immunotherapy in a preclinical model of advanced-stage ovarian cancer. Clin. Cancer Res. *25*, 1624–1638.
24. Roby, K.F., Taylor, C.C., Sweetwood, J.P., Cheng, Y., Pace, J.L., Tawfik, O., Persons, D.L., Smith, P.G., and Terranova, P.F. (2000). Development of a syngeneic mouse model for events related to ovarian cancer. Carcinogenesis *21*, 585–591.
25. Song, M., Yeku, O.O., Rafiq, S., Purdon, T., Dong, X., Zhu, L., Zhang, T., Wang, H., Yu, Z., Mai, J., et al. (2020). Tumor derived UBR5 promotes ovarian cancer growth and metastasis through inducing immunosuppressive macrophages. Nat. Commun. *11*, 6298.
26. Steitz, A.M., Steffes, A., Finkernagel, F., Unger, A., Sommerfeld, L., Jansen, J.M., Wagner, U., Graumann, J., Müller, R., and Reinartz, S. (2020). Tumor-associated macrophages promote ovarian cancer cell migration by secreting transforming growth factor beta induced (TGFBI) and tenascin C. Cell Death Dis. *11*, 249.
27. Hume, D.A., and MacDonald, K.P. (2012). Therapeutic applications of macrophage colony-stimulating factor-1 (CSF-1) and antagonists of CSF-1 receptor (CSF-1R) signaling. Blood *119*, 1810–1820.
28. Stafford, J.H., Hirai, T., Deng, L., Chernikova, S.B., Urata, K., West, B.L., and Brown, J.M. (2016). Colony stimulating factor 1 receptor inhibition delays recurrence of glioblastoma after radiation by altering myeloid cell recruitment and polarization. Neuro Oncol. *18*, 797–806.
29. Anderson, A.C., Joller, N., and Kuchroo, V.K. (2016). Lag-3, Tim-3, and TIGIT: co-inhibitory receptors with specialized functions in immune regulation. Immunity *44*, 989–1004.
30. Togashi, Y., Shitara, K., and Nishikawa, H. (2019). Regulatory T cells in cancer immunosuppression - implications for anticancer therapy. Nat. Rev. Clin. Oncol. *16*, 356–371.
31. Cannarile, M.A., Weisser, M., Jacob, W., Jegg, A.M., Ries, C.H., and Rüttinger, D. (2017). Colony-stimulating factor 1 receptor (CSF1R) inhibitors in cancer therapy. J. Immunother. Cancer *5*, 53.
32. Jeannin, P., Paolini, L., Adam, C., and Delneste, Y. (2018). The roles of CSFs on the functional polarization of tumor-associated macrophages. FEBS J. *285*, 680–699.
33. Ayantunde, A.A., and Parsons, S.L. (2007). Pattern and prognostic factors in patients with malignant ascites: a retrospective study. Ann. Oncol. *18*, 945–949.
34. Burges, A., Wimberger, P., Kümper, C., Gorbounova, V., Sommer, H., Schmalfeldt, B., Pfisterer, J., Lichinitser, M., Makhson, A., Moiseyenko, V., et al. (2007). Effective relief of malignant ascites in patients with advanced ovarian cancer by a trifunctional anti-EpCAM x anti-CD3 antibody: a phase I/II study. Clin. Cancer Res. *13*, 3899–3905.
35. Seimetz, D., Lindhofer, H., and Bokemeyer, C. (2010). Development and approval of the trifunctional antibody catumaxomab (anti-EpCAM x anti-CD3) as a targeted cancer immunotherapy. Cancer Treat. Rev. *36*, 458–467.
36. Monk, B.J., Minion, L.E., and Coleman, R.L. (2016). Anti-angiogenic agents in ovarian cancer: past, present, and future. Ann. Oncol. *27*, i33–i39.
37. Pfisterer, J., Shannon, C.M., Baumann, K., Rau, J., Harter, P., Joly, F., Sehouli, J., Canzler, U., Schmalfeldt, B., Dean, A.P., et al. (2020). Bevacizumab and platinum-based combinations for recurrent ovarian cancer: a randomised, open-label, phase 3 trial. Lancet Oncol. *21*, 699–709.
38. Martinez-Quintanilla, J., Seah, I., Chua, M., and Shah, K. (2019). Oncolytic viruses: overcoming translational challenges. J. Clin. Invest. *129*, 1407–1418.
39. Nakao, S., Arai, Y., Tasaki, M., Yamashita, M., Murakami, R., Kawase, T., Amino, N., Nakatake, M., Kurosaki, H., Mori, M., et al. (2020). Intratumoral expression of IL-7 and IL-12 using an oncolytic virus increases systemic sensitivity to immune checkpoint blockade. Sci. Transl. Med. *12*, eaax7992.
40. Andtbacka, R.H., Kaufman, H.L., Collichio, F., Amatruda, T., Senzer, N., Chesney, J., Delman, K.A., Spitler, L.E., Puzanov, I., Agarwala, S.S., et al. (2015). Talimogene Laherparepvec improves durable response rate in patients with advanced melanoma. J. Clin. Oncol. *33*, 2780–2788.
41. Yin, M., Li, X., Tan, S., Zhou, H.J., Ji, W., Bellone, S., Xu, X., Zhang, H., Santin, A.D., Lou, G., et al. (2016). Tumor-associated macrophages drive spheroid formation during early transcoelomic metastasis of ovarian cancer. J. Clin. Invest. *126*, 4157–4173.
42. Liu, Z., Ravindranathan, R., Kalinski, P., Guo, Z.S., and Bartlett, D.L. (2017). Rational combination of oncolytic vaccinia virus and PD-L1 blockade works synergistically to enhance therapeutic efficacy. Nat. Commun. *8*, 14754.
43. Rein, D.T., Volkmer, A., Beyer, I.M., Curiel, D.T., Janni, W., Dragoi, A., Hess, A.P., Maass, N., Baldus, S.E., Bauerschmitz, G., et al. (2011). Treatment of chemotherapy resistant ovarian cancer with a MDR1 targeted oncolytic adenovirus. Gynecol. Oncol. *123*, 138–146.
44. Zhang, Y.Q., Tsai, Y.C., Monie, A., Wu, T.C., and Hung, C.F. (2010). Enhancing the therapeutic effect against ovarian cancer through a combination of viral oncolysis and antigen-specific immunotherapy. Mol. Ther. *18*, 692–699.
45. Pitt, J.M., Vétizou, M., Daillère, R., Roberti, M.P., Yamazaki, T., Routy, B., Lepage, P., Boneca, I.G., Chamaillard, M., Kroemer, G., et al. (2016). Resistance mechanisms to

immune-checkpoint blockade in cancer: tumor-intrinsic and -extrinsic factors. Immunity *44*, 1255–1269.

46. Kalbasi, A., and Ribas, A. (2020). Tumour-intrinsic resistance to immune checkpoint blockade. Nat. Rev. Immunol. *20*, 25–39.

47. Bejarano, L., Jordão, M.J.C., and Joyce, J.A. (2021). Therapeutic targeting of the tumor microenvironment. Cancer Discov. *11*, 933–959.

48. Sharma, P., and Allison, J.P. (2015). Immune checkpoint targeting in cancer therapy: toward combination strategies with curative potential. Cell *161*, 205–214.

49. Nguyen, H.M., Bommareddy, P.K., Silk, A.W., and Saha, D. (2021). Optimal timing of PD-1 blockade in combination with oncolytic virus therapy. Semin. Cancer Biol. https://doi.org/10.1016/j.semcancer.2021.05.019.

50. Shi, G., Yang, Q., Zhang, Y., Jiang, Q., Lin, Y., Yang, S., Wang, H., Cheng, L., Zhang, X., Li, Y., et al. (2019). Modulating the tumor microenvironment via oncolytic viruses and CSF-1R inhibition synergistically enhances anti-PD-1 immunotherapy. Mol. Ther. *27*, 244–260.

51. Huang, R.Y., Eppolito, C., Lele, S., Shrikant, P., Matsuzaki, J., and Odunsi, K. (2015). LAG3 and PD1 co-inhibitory molecules collaborate to limit $CD8^+$ T cell signaling and dampen antitumor immunity in a murine ovarian cancer model. Oncotarget *6*, 27359–27377.

52. Huang, R.Y., Francois, A., McGray, A.R., Miliotto, A., and Odunsi, K. (2017). Compensatory upregulation of PD-1, LAG-3, and CTLA-4 limits the efficacy of single-agent checkpoint blockade in metastatic ovarian cancer. Oncoimmunology *6*, e1249561.